The effect of manufacture and assembly joining methods on stiffened panel performance

THE EFFECT OF MANUFACTURE AND ASSEMBLY JOINING METHODS ON STIFFENED PANEL PERFORMANCE

C. Harley, D. Quinn, T. Robinson and S. Goel

1. School of Mechanical & Aerospace Engineering, Queen's University Belfast, United Kingdom

ABSTRACT

This paper describes the simulation of representative aircraft wing stiffened panels under axial compression loading, to determine the effects of varying the manufacturing shape and assembly joining methods on stiffened panel performance. T-stiffened and Z-stiffened panels are modelled in Abaqus simulating integral, co-cured and mechanically fastened joints. The panels are subject to an edge compressive displacement along the stiffener axis until failure and the ultimate failure load and buckling performance is assessed for each. Integral panels consistently offer the highest performance. Co-cured panels demonstrate reduced performance (3-5% reduction in ultimate load relative to integral) caused by localised cohesive failure and skin-stiffener separation. The mechanically fastened panels are consistently the weakest joint (19-25% reduction in ultimate load relative to integral) caused primarily by inter-rivet buckling between fasteners.

KEYWORDS: Composite, Stiffened Panel, Compression

1. INTRODUCTION

The use of composite materials in the aerospace industry is ubiquitous due to enhanced structural performance and weight reduction. Stiffened panels are key structural members of an aircraft thereby requiring significant attention in design and manufacture. A typical stiffened panel will have longitudinal (stringer) or transverse (frame) members to support the skin in the form of sheet material. Composite stiffened panels are commonly found in aircraft structures throughout the fuselage and wing structure where compression and buckling strength are important design considerations. Skin-stiffener joint strength is critical to the structural performance of the part and understanding how stiffener shape and joining method influence joint strength and the subsequent load carrying capabilities of the stiffened panel is the key motivation to this work.

1.1 Stiffened Panel Design

Stiffened panels traditionally comprise a prismatic stiffener attached to a uniform thickness skin plate. The stiffener shape can vary depending on the type of loading, static strength requirements, and in some cases the choice of skin-stiffener assembly method. There have been multiple studies throughout literature on the effects of stiffener shape on compression buckling performance and ultimate static strength. For example, Kong *et al.* [1] compared the post-buckling strength and failure under axial compression of blade, I and hat stiffeners using nonlinear finite element analysis to find that the compressive and post-buckling strength increases in strength from blade, I to hat respectively and the torsional stiffness of the stiffener was found to be the primary contributing factor. Other

researchers have studied composite hat-stiffened panels to prove their superiority under compression loading including analysing pull off tests and stiffening effects on a plate [2-4]. However the additional effect of various skin-stiffener joining methods, and their potential interaction with stiffener cross sectional shape, has yet to be fully understood.

1.2 Manufacture of Composite Stiffened Panels

Stiffeners can be integral, co-cured, co-bonded or mechanically fastened to the skin. Integral stiffened panels are manufactured as one part, in which the stiffener and skin are formed from continuous plies. Co-cure joining methods consist of the skin and stiffener curing simultaneously to create a continuous interface joint, which can be more cost effective compared to co-bonding, which allows the skin and stiffener to cure independently before bonding using an adhesive layer. Mechanical fastening again allows the skin and stiffener to be manufactured separately, but joined using fasteners at discrete points on the skin-stiffener interface.

Skin-stiffener joint failure through debonding is a crucial failure mechanism in composite stiffened panels under compression loading. Kim *et al.* [5] compared the performance of composite hat-stiffened panels with varying manufacturing joining methods, using co-curing, co-bonding and secondary bonding to compare the strengths. Pull-off tests performed to assess transverse joint strength established that secondary bonding was the weakest of the joints studied, with joint strength increasing from co-bonding to co-curing, and co-curing exhibiting no skin-stiffener debond. Stiffened panels however have not been analysed considering the combined effects of stiffener shape and joining methods on panel strength.

The stiffener shape and joint manufacturing and assembly method will provide the skin with varying degrees of torsional rigidity along its supported edges. As a result, the different combinations may induce unique responses under compression loading and potentially exhibit different failure modes. For example, Li *et al.* [6] studied the buckling modes of stiffened panels under compression due to different stiffener types and edge constraints. When simulating reduced stiffener rigidity at the edge of the skin, buckling occurs at the edge of the skin bay where the stiffener is located, as opposed to simulating an increase in stiffener rigidity where buckling occurs in the middle of the skin bay.

1.3 Analysis and Design of Composite Structures

For composite structures to be designed and certified, a large number of experimental material coupon and structural detail characterisation tests are required, which capture the complex interactions, establish material properties and design allowables. Expansion of experimental analysis using validated numerical virtual testing techniques (simulation of Compression After Impact tests for example) have the potential to yield a more efficient and more optimal design process by considering an enlarged design envelope capable of representing the laminate structural response within the true aircraft environment.

The static strength performance and behaviour of composite stiffened panels and uniform thickness plates under axial compression or transverse impact loading can be predicted successfully using various numerical analysis [7-11] or analytical modelling methods [12, 13]. Capturing laminate damage behaviour is one of the key challenges and the selection of appropriate constitutive modelling

methods, failure criteria and damage modelling are crucial for accurate results when modelling compression and impact on composite plates [14]. To date, methods for predicting compressive strength and impact damage have been successful in predicting the non-linear response of composite structures modelled under simple experimental test conditions (for example low velocity impact of a simply supported or clamped flat square plate by a rigid impactor). However, these simulation conditions are not typically representative of the real-life structures and progression of these modelling capabilities to enable characterisation and understanding of the composite structural response within a true aircraft environment is required.

1.4 Simulation Intent for Composite Design

The long term objective of this work is to use the concept of Simulation Intent to aid the simulation of composite panel analysis by providing a framework required to facilitate multi-level modelling and automation [15]. The use of Simulation Intent will be investigated as a means to automate the workflows between multi-fidelity models and to define the relationships between the different simulation models required to actively capture and account for truly representative boundary conditions during the design process. Creating Compression After Impact analysis models with variable boundary conditions capable of simulating variable stiffener shape and joining methods will develop an understanding of possible limitations and conservatism in current stiffened panel designs and produce more damage tolerant and weight efficient solutions.

The remainder of this paper describes the initial phase of this work, investigating the effect of varying stiffener cross sectional shape and panel joining methods using commercial FEA software Abaqus. Simulations are performed on pristine panels without the inclusion of localised joint damage, to determine the effects of the manufacturing choices for stiffener shape and joining methods on stiffened panel compression strength.

2. METHODOLOGY

2.1 Stiffened Panel Idealisation

The structural model consists of a single stiffener with a full skin bay on either side. Two stiffener cross sectional configurations are modelled; inverted T and Z sections as shown in Figure 1 (a) and (c) respectively. The geometries are representative of typical aircraft wing stiffened panels, with a 600mm panel length typical of wing rib pitch and a panel width of 340mm typical of stiffener pitch, with additional dimensions detailed in Figure 1. To assess the influence of cross section shape on panel performance and behaviour the cross sectional area of both stiffeners are held constant.

The stiffened panel skin, flanges and web sections are modelled separately using standard continuum SC8R deformable shell elements and meshed with an element length of 4mm along feature edges, with the mesh of the Z stiffened panel illustrated in Figure 1(d). Continuum shell elements are used to capture the through-thickness effects for composites laminates and to assess delamination damage through modelling two-sided contact between the skin and stiffener.

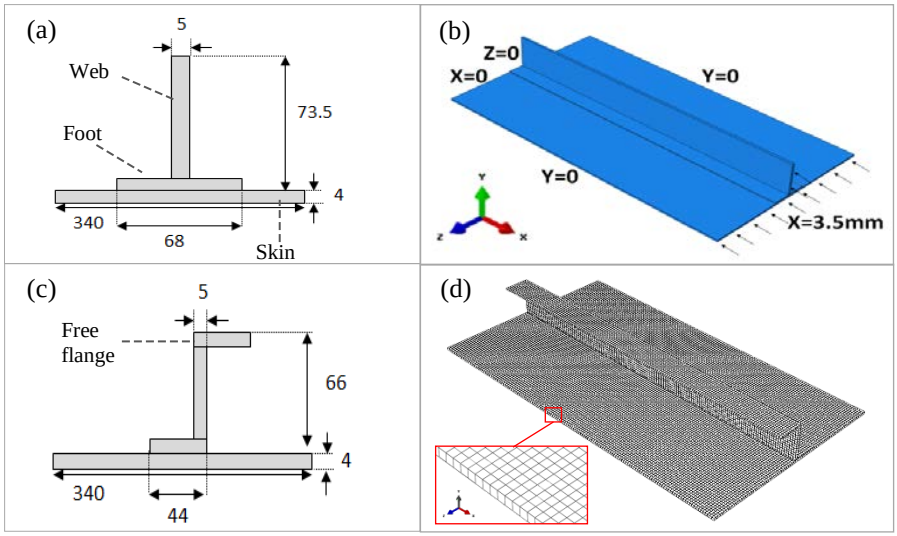

Figure 1.(a) T-stiffened panel geometry (b) T-stiffened panel with boundary conditions (c) Z-stiffened panel geometry (d) Z-stiffened panel mesh

2.2 Joint Interface

Three manufacturing joining idealisations, Integral, Co-cured and Mechanical Fastening (Table 1), are simulated for both stiffener shapes to determine the effects of manufacturing joining options on stiffened panel compression performance. The interface between the skin and stiffener foot is varied according to manufacturing option, using either rigid beam elements (Multi-Pont Constraints) or cohesive elements as described in Table 1. The individual stiffener elements (web, foot and free flange) are connected using Multi-Point Constraints in a manner that models a continuous rigid connection between the various stiffener elements.

Table 1. Stiffener Joining Idealisations for T-stiffener

	Stiffener Manufacturing and Assembly Idealisation		
	Integral	Co-Cure	Mechanical Fastener
FE Equivalent Representation	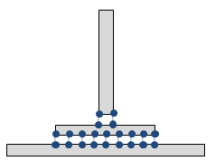	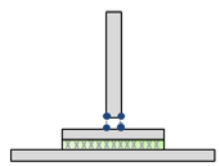	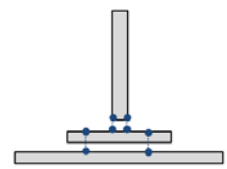
	MPC connecting skin top surface nodes and stiffener foot bottom surface nodes degrees of freedom.	Cohesive Interaction between skin and stiffener foot adjacent surfaces, defining damage initiation and evolution fracture energies.	Single point MPCs connecting single skin nodes and stiffener foot nodes at fastener locations. Fastener pitch is 50mm.

Cohesive joints are modelled in the co-cure idealisation using the cohesive surface interaction to simulate interlaminar interaction and delamination. Cohesive failure is captured using maximum nominal stress damage criterion for

damage initiation, considering mode I and mode II fracture energies to define interface damage criteria. The mixed mode Benzeggagh-Kenane criterion [16] is used for damage evolution considering representative fracture energies [17].

2.3 Laminate Modelling

The composite stiffened panels are modelled as assemblies of orthotropic mid-plane shells, representative of the stiffener and skin section stacking sequences. The thermoplastic material consists of Carbon fibres and a Polyphenylene Sulfide (PPS) matrix, with representative strength and stiffness material properties [18, 19]. Table 2 details the ply and stacking sequence information for each skin and stiffener element.

Table 2. Section Ply and Stacking Sequence

Section	Number of Plies	Ply Thickness (m)	Stacking Sequence
Skin	16	0.00025	$[+45/-45/0_2/90/+45/-45/0]$
Foot and Free Flange	10	0.00025	[0/90/0/+45/-45/0/+45/-45/0/90]
Web	20	0.00025	$[0/90/0/+45/-45/0/+45/-45/0/90]_s$

Laminate failure is modelled using the interactive Hashin failure criteria to capture localised failure in the fibre or matrix due to tension or compression [20]. The material failure strengths are defined from literature [18, 19] and failure occurs when the failure index for each mode is greater than or equal to 1.

2.4 Boundary Conditions

The panel is loaded in compression along the stiffener axis by enforcing a 3.5mm edge displacement along the panel lateral edge, as illustrated on the T-stiffened panel in Figure 1(b), with equivalent translation fixed on the opposite lateral edge. Out-of-plane displacement is constrained along all lateral and longitudinal edges to provide simply supported panel edge conditions.

3. RESULTS

A total of six simulations were performed for both T and Z stiffened panels with various joining methods. The ultimate compressive failure load for each configuration is presented in Table 3, including the variation in load carrying performance relative to the integral T and Z stiffeners. A comparison of the effects of manufacturing joining and shape idealisations on stiffened panel performance is detailed in the following sections.

Table 3. Ultimate Compressive Failure Load

	T-Stiffened Panel			**Z-Stiffened Panel**		
	Integral	*Co-Cure*	*Fastener*	*Integral*	*Co-Cure*	*Fastener*
Ultimate Compressive Load (kN)	565	535	460	520	504	426
% Variation wrt T Integral	-	5	19	8	11	25
% Variation wrt Z Integral				-	3	18

3.1 Influence of Manufacturing Joining Methods

The Load-Displacement plot for the integral, co-cure and mechanical fastening joining methods of the T-stiffened panel are illustrated in Figure 2(a). The out-of-plane displacement contours (Figure 2(b), 2(c) and 2(d)) illustrate local buckling modes and matrix tension failure contours (Figure 3(a), 3(b) and 3(c)) are also shown to illustrate the location of laminate material failure.

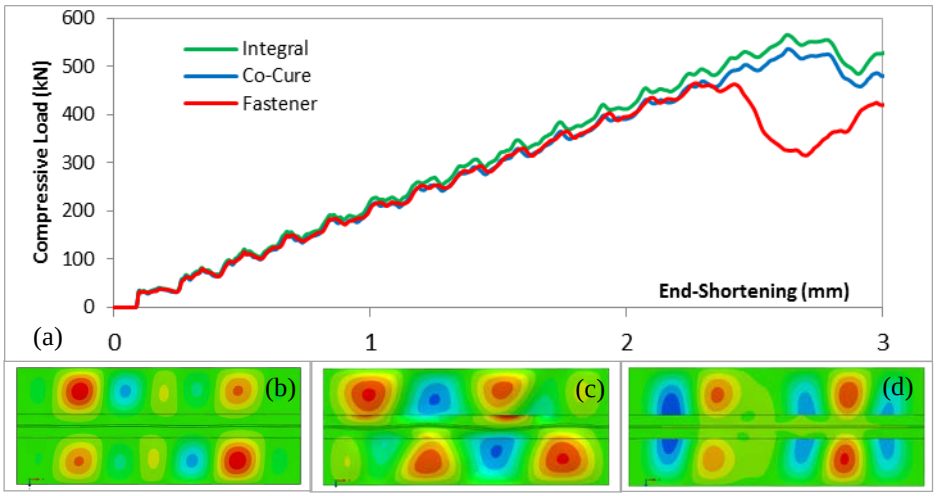

Figure 2. (a) Load-End-Shortening Plot for the T-stiffened panel. Out-of-plane displacement contour for (b) Integral T-stiffened panel (c) Co-Cure T-stiffened panel (d) Mechanically Fastened T-stiffened panel

The integral T-stiffened panel failed at 565kN, due to localised matrix tension failure on the skin bay as shown in Figure 3(a). Prior to failure the panel began buckling in the skin bay at 87% ultimate load, producing 4 uniform asymmetric buckle half waves on each skin bay at the point of failure, and the out of plane displacement contour of the panel at failure is shown in Figure 2(b). The localised matrix tension failure corresponds to the buckling wave locations. The panel exhibits no material failure on the stiffener at ultimate load and the skin-stiffener joint remains intact throughout.

The co-cure T-stiffened panel failed at 535kN (5% lower than the integral panel) exhibiting localised matrix tension failure on the skin bay, Figure 3(b), and localised separation of the skin and stiffener, Figure 3(e), in which the skin-foot interface damage is illustrated in Figure 3(d). The stiffener exhibited no material failure of any form at ultimate load. The panel demonstrated skin bay buckling prior to failure at 85% ultimate load, and produced 4 half waves on both skin bays. Skin-stiffener bond failure and localised separation at the ultimate failure load resulted in irregular buckling waves forming under the stiffener foot as illustrated in Figure 2(c).

The mechanically fastened T-stiffened panel failed at 460kN (19% lower than the integral panel) exhibiting localised matrix tension failure on the skin bay and no material failure on the stiffener, similar to the previous two joining methods. The panel demonstrated skin bay buckling prior to failure at 81% ultimate load, displaying 4 irregular half waves on both skin bays (Figure 2(d)). Localised skin buckling and skin-stiffener separation is also present under the stiffener foot between fastener locations (Figure 3(f)).

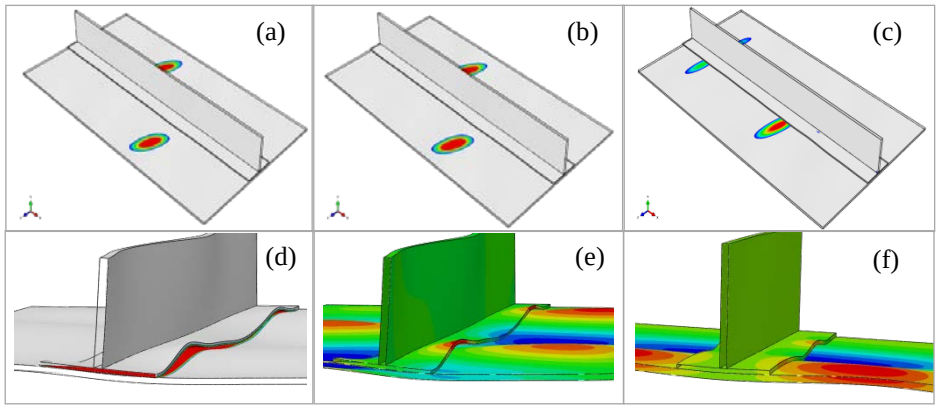

Figure 3. Hashin Matrix Tension Failure Contour for (a) Integral T-stiffened panel (b) Co-Cure T-stiffened panel (c) Mechanically Fastened T-stiffened panel (d) Cohesive interface failure for Co-Cure T-stiffened panel (e) Foot-stiffener separation for Co-Cure T-stiffened panel (f) Foot-stiffener separation for Mechanically Fastened T-stiffened panel

The integral structure is the strongest joining method of the three analysed, and mechanical fastening the predicted weakest joint. All three panels demonstrate localised skin matrix tension failure attributed to the formation of skin buckling waves, with high bending stresses at the crest of the buckle waves triggering material failure. The key difference in observed behaviour between the panels is the skin buckling performance and the potential influence of the skin-stiffener joint in driving such buckling behaviour.

The buckling load of the co-cured panel is lower than that of the integral panel. Reduction in the cohesive strength, and eventual separation, of the skin-stiffener interface appears to have initiated local skin buckling and subsequent material failure at an earlier stage. The localised breakdown of the skin-stiffener joint has potentially reduced the level of torsional rigidity and support offered by the stiffener, thus causing skin buckling and subsequent panel failure to occur at a reduced load. Similarly for the mechanically fastened panel, initial skin buckling is triggered at a much lower load than the integral panel. Observation of the buckling modes suggest that the level of torsional support offered by the stiffener is not as high as that of an integral or co-cured joint, indicative of the stiffener being joined at discrete points as opposed to a continuous joint. Furthermore, support of the stiffener to the skin is further compromised by local inter-rivet buckling between the fasteners attributed to the relatively large fastener pitch of 50mm.

3.2 Influence of Stiffener Cross Sectional Shape

The Load-Displacement plots for the co-cured and mechanically fastened T and Z-stiffened panels are presented in Figure 4(a). The out-of-plane displacement contours (Figure 4(b) and 4(c)) illustrate local buckling modes and matrix tension failure contours (Figure 5(a) and 5(b)) are also shown to illustrate the location of laminate material failure.

The integral Z-stiffened panel failed at 520kN (8% lower than the integral T-stiffened panel), due to localised matrix tension failure on stiffener free flange and skin bay. Prior to failure the panel began buckling at 70% of ultimate load exhibiting five uniform buckle half waves on one skin bay, similar to the co-cure

shown in Figure 4(b). The panel exhibits no matrix tension failure on the stiffener foot and web at the point of failure and the skin-stiffener joint remains intact.

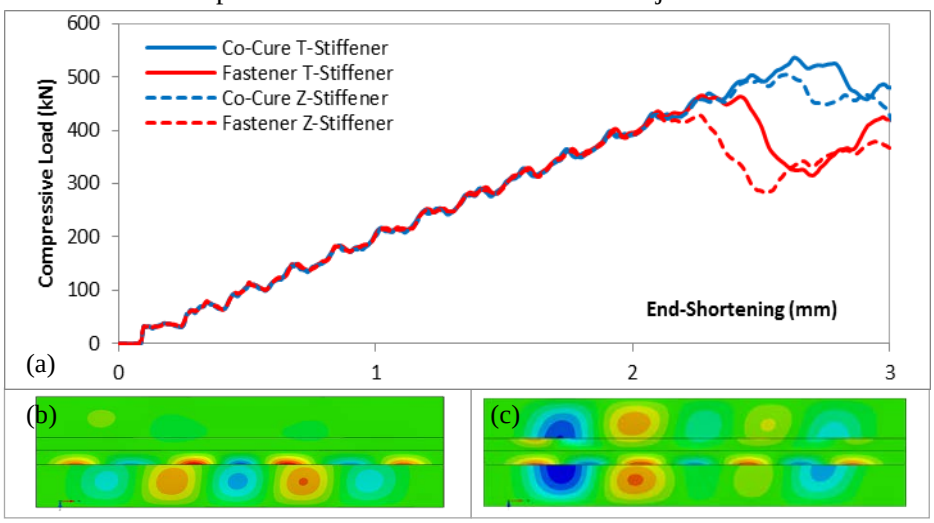

Figure 4. (a) Load-End-Shortening Plot comparing stiffener shape. Out-of-plane displacement for (b) Co-Cure Z-stiffened panel (c) Mechanically Fastened Z-stiffened panel

The co-cure Z-stiffened panel failed at 504kN (6% lower than the co-cured T-stiffened panel and 3% lower than the integral Z-stiffened panel). Prior to failure the buckling of the stiffener free flange occurred at 69% ultimate load, and buckling of one skin bay into five buckle half waves at 99% of ultimate load, Figure 4(b). Panel failure is due to localised matrix tension failure on the free flange and skin bay corresponding to buckling wave locations, Figure 5(a), accompanied by localised skin-stiffener separation. The panel exhibits no material failure on the stiffener foot or web at failure.

The mechanically fastened Z-stiffened panel failed at 426kN (7% lower than the mechanically fastened T-stiffened panel and 18% lower than the integral Z-stiffened panel), due to localised matrix tension failure on the free flange and skin bay corresponding to buckling wave locations (Figure 5(b)). Prior to failure the panel began buckling at 68% of ultimate load in the skin bay and stiffener free flange, and at the point of failure exhibited five buckle half waves on the skin bays, as illustrated in Figure 4(c). The panel exhibits no material failure on the stiffener foot or web at the point of failure.

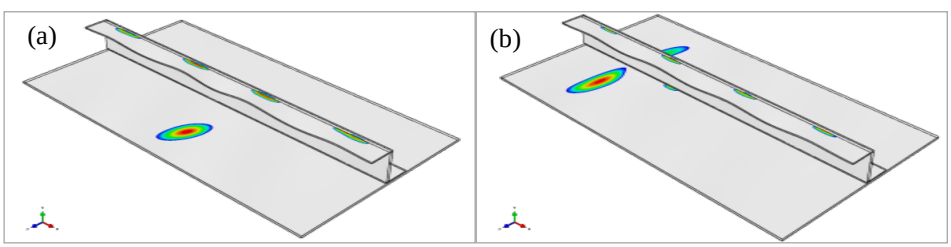

Figure 5. Hashin Matrix Tension Failure Contour for (a) Co-Cure Z-stiffened panel (e) Mechanically Fastened Z-stiffened panel

For all joining process considered the T-stiffened panel is stronger under axial compression loading in comparison to the Z-stiffened panel. Comparing the out-of-plane buckling modes highlights a key difference in the panel behaviour. Buckling of the T-stiffened panels was generally confined to the skin bays on

either side of the stiffener, whereas the Z-stiffened panels demonstrate buckling of the stiffener free flange in addition to skin buckling. The T-stiffened panels exhibit reduced magnitude and number of buckling waves compared to the skin and free-flange out of plane displacements of the Z-stiffened panels. This suggests a greater resistance to out of plane bending of the T-stiffened panels compared to the Z-stiffened panels. Furthermore, when considering the co-cure joining methods, the T-stiffened panels demonstrate comparable out-of-plane displacements on both skin bays either side of the stiffener (Figure 2(c)), however the Z-stiffened panel differs in that the buckling is limited on one skin bay before the other, as illustrated in Figure 4(b). This suggests the variation in panel buckling performance and the reduction in compressive load carrying capabilities between T-stiffener and Z-stiffener appears to be linked to the skin and stiffener out-of-plane buckling behaviour. The analysis suggests the Z-stiffener exhibits a lower torsional rigidity in comparison to the T-stiffener under compression loading.

With regards to panel failure mechanisms there is also a distinct difference between the T and Z-stiffened panels. For the T-stiffened panels localised matrix tension failure at skin buckling locations is the primary failure mechanism, with no material failure exhibited in the stiffener sections. Whereas the Z-stiffened panels exhibit localised matrix tension failure at the free flange and skin bay buckling locations and no material failure on the stiffener foot or web sections at the point of failure under compression loading. Initial local buckling of the free flange and subsequent localised matrix tension failure appears to have triggered earlier failure of the Z-stiffener in comparison to the T-stiffener.

4. CONCLUSIONS

This paper presented six case studies of varying stiffened panel configurations and joining methods to determine the effect of stiffener manufacture or assembly choices on stiffened panel compressive strength and buckling behaviour. T and Z-stiffened panels were analysed in Abaqus considering integral, co-cured and mechanically fastened manufacturing options. The key conclusions of this study are:

I. For both the T-stiffened panel and Z-stiffened panel the integral joining method is the strongest under compression loading. Co-cured panels demonstrated lower ultimate strength, potentially attributed to localised cohesive failure and skin-stiffener separation which triggered initial skin buckling and subsequent panel failure at lower loads. The mechanically fastened stiffened panels are the weakest under compression loading for both T-stiffeners and Z-stiffeners, with localised inter-rivet buckling compromising the skin-stiffener joint and thus affecting the level of support offered by the stiffener to the skin. The magnitudes of the variation in strength due to the three joining processes are similar for T-stiffener and Z-stiffener panels.

II. T-stiffened panels are consistently stronger than Z-stiffened panels under compression loading. Variation in the skin buckling patterns suggests the Z-stiffener offers reduced torsional rigidity to the skin, and thus reduces the skin resistance to out of plane bending.

III. Failure mechanisms on all panels correspond to matrix tension failure occurring at buckle wave crest locations. However, subsequent material failure occurs on the skin bays alone for the T-stiffened panels and the Z-stiffened panels also display local buckling of the stiffener free flange elements. This triggers material failure of the stiffener free flange and ultimately contributes to the reduced load carrying ability of the Z-stiffened panels.

IV. The interaction of stiffener cross section shape and joining methods can influence the level of support the skin and stiffener contribute to each other. The skin out-of-plane resistance is driven by the combination of stiffener shape and joining method. This may affect not only panel axial compression performance, but any loading scenario where skin out-of-plane behaviour is critical such as transverse impact loading.

5. REFERENCES

[1] B. Kong, P. Chen and Y. Chen. Post-buckling failure evaluation method of integrated composite stiffened panels under uniaxial compression. *Fuhe Cailiao Xuebao/Acta Materiae Compositae Sinica)*, Vol.31 (2014), 765-771.

[2] R. H. Martin. Local fracture mechanics analysis of stringer pull-off and delamination in a post-buckled compression panel. *Applied Composite Materials*, Vol.3(4) (1996), 249-264.

[3] J. Li, T. K. O'Brien and C. Q. Rousseau. Test and analysis of composite hat stringer pull-off test specimens. *Journal of the American Helicopter Society*, Vol.42(4) (1997), 350-357.

[4] O. Funatogawa, I. Kimpara and M. Takehana. On the stiffening effect of hat-shaped stiffeners on a plate. *Naval Architecture and Ocean Engineering*, Vol.18 (1980), 115-131.

[5] G. Kim, J. Choi and J. Kweon. Manufacture and performance evaluation of the composite hat-stiffened panel. *Composite Structures*, Vol.92(9) (2010), 2276-2284.

[6] C. Li and Z. Wu. Buckling of 120° stiffened composite cylindrical shell under axial compression - experiment and simulation. *Composite Structures*, Vol.128 (2015), 199-206.

[7] C. S. Lopes, P. P. Camanho, Z. Gürdal, P. Maimí and E. V. González. Low-velocity impact damage on dispersed stacking sequence laminates. part II: Numerical simulations. *Composites Sci. Technol.* Vol.69(7-8) (2009), 937-947.

[8] M. V. Donadon, L. Iannucci, B. G. Falzon, J. M. Hodgkinson and S. F. M. de Almeida. A progressive failure model for composite laminates subjected to low velocity impact damage. *Computers and Structures*, Vol.86(11-12) (2008), 1232-1252.

[9] P. W. Harper and S. R. Hallett. Cohesive zone length in numerical simulations of composite delamination. *Eng. Fract. Mech.* Vol.75(16) (2008), 4774-4792.

[10] R. Borg, L. Nilsson and K. Simonsson. Modeling of delamination using a discretized cohesive zone and damage formulation. *Composites Sci. Technol.* Vol.62(10-11) (2002), 1299-1314.

[11] A. Faggiani and B. G. Falzon. Predicting low-velocity impact damage on a stiffened composite panel. *Composites Part A: Applied Science and Manufacturing*, Vol.41(6) (2010), 737-749.

[12] S. Abrate. Modeling of impacts on composite structures. *Composite Structures*, Vol.51(2) (2001), 129-138.

[13] R. Olsson, M. V. Donadon and B. G. Falzon. Delamination threshold load for dynamic impact on plates. *Int. J. Solids Structures*, Vol.43(10) (2006), 3124-3141.

[14] A. C. Orifici, I. Herszberg and R. S. Thomson. Review of methodologies for composite material modelling incorporating failure. *Composite Structures*, Vol.86(1-3) (2008), 194-210.

[15] D. C. Nolan, C. M. Tierney, C. G. Armstrong and T. T. Robinson. Defining simulation intent. *CAD Computer Aided Design, Vol.59 (2015)*, 50-63.

[16] M. L. Benzeggagh and M. Kenane. Measurement of mixed-mode delamination fracture toughness of unidirectional glass/epoxy composites with mixed-mode bending apparatus. *Composites Sci. Technol.* Vol.56(4) (1996), 439-449.

[17] C. S. Lopes, P. P. Camanho, Z. Gürdal and B. F. Tatting. Progressive failure analysis of tow-placed, variable-stiffness composite panels. *Int. J. Solids Structures*, Vol.44(25-26) (2007), 8493-8516.

[18] J. Reeder, S. Kyongchan and P. B. Chunchu, " Postbuckling and Growth of Delaminations in Composite Plates Subjected to Axial Compression," *American Institute of Aeronautics and Astronautics*, 2002.

[19] G. Z. Voyiadjis and P. I. Kattan. Mechanics of composite materials with MATLAB. *Mechanics of Composite Materials with MATLAB*, 2005, 1-336.

[20] 6. 1. Abaqus, "ABAQUS Analysis User's Manual © 2011 DASSULT SYSTEMES" .